Theoretical investigation of compact couplers between dielectric slab waveguides and two-dimensional metal-dielectric-metal plasmonic waveguides

Georgios Veronis and Shanhui Fan

Department of Electrical Engineering, Stanford University, Stanford, California 94305
gveronis@stanford.edu

Abstract: We theoretically investigate the properties of compact couplers between high-index contrast dielectric slab waveguides and two-dimensional metal-dielectric-metal subwavelength plasmonic waveguides. We show that a coupler created by simply placing a dielectric waveguide terminated flat at the exit end of a plasmonic waveguide can be designed to have a transmission efficiency of ∼70% at the optical communication wavelength. We also show that the transmission efficiency of the couplers can be further increased by using optimized multisection tapers. In both cases the transmission response is broadband. In addition, we investigate the properties of a Fabry-Perot structure in which light is coupled in and out of a plasmonic waveguide sandwiched between dielectric waveguides. Finally, we discuss potential fabrication processes for structures that demonstrate the predicted effects.

© 2007 Optical Society of America

OCIS codes: (130.2790) Guided waves; (240.6680) Surface plasmons; (130.3120) Integrated optics devices.

References and links

1. J. Takahara, S. Yamagishi, H. Taki, A. Morimoto, and T. Kobayashi, "Guiding of a one-dimensional optical beam with nanometer diameter," Opt. Lett. **22,** 475–477 (1997).
2. J. C. Weeber, A. Dereux, C. Girard, J. R. Krenn, and J. P. Goudonnet, "Plasmon polaritons of metallic nanowires for controlling submicron propagation of light," Phys. Rev. B **60,** 9061–9068 (1999).
3. J. R. Krenn, B. Lamprecht, H. Ditlbacher, G. Schider, M. Salerno, A. Leitner, and F. R. Aussenegg, "Non-diffraction-limited light transport by gold nanowires," Europhys. Lett. **60,** 663–669 (2002).
4. M. L. Brongersma, J. W. Hartman, and H. A. Atwater, "Electromagnetic energy transfer and switching in nanoparticle chain arrays below the diffraction limit," Phys. Rev. B **62,** R16356–R16359 (2000).
5. S. A. Maier, P. G. Kik, H. A. Atwater, S. Meltzer, E. Harel, B. E. Koel, and A. A. G. Requicha, "Local detection of electromagnetic energy transport below the diffraction limit in metal nanoparticle plasmon waveguides," Nat. Mater. **2,** 229–232 (2003).
6. S. I. Bozhevolnyi, V. S. Volkov, E. Devaux, and T. W. Ebbesen, "Channel plasmon-polariton guiding by subwavelength metal grooves," Phys. Rev. Lett. **95,** 046802 (2005).
7. E. N. Economou, "Surface plasmons in thin films," Phys. Rev. **182,** 539–554 (1969).
8. K. Tanaka and M. Tanaka, "Simulations of nanometric optical circuits based on surface plasmon polariton gap waveguide," Appl. Phys. Lett. **82,** 1158–1160 (2003).
9. F. Kusunoki, T. Yotsuya, J. Takahara, and T. Kobayashi, "Propagation properties of guided waves in index-guided two-dimensional optical waveguides," Appl. Phys. Lett. **86,** 211101 (2005).

10. G. Veronis and S. Fan, "Guided subwavelength plasmonic mode supported by a slot in a thin metal film," Opt. Lett. **30,** 3359–3361 (2005).
11. L. Liu, Z. Han, and S. He, "Novel surface plasmon waveguide for high integration," Opt. Express **13,** 6645-6650 (2005).
12. D. F. P. Pile, T. Ogawa, D. K. Gramotnev, Y. Matsuzaki, K. C. Vernon, K. Yamaguchi, T. Okamoto, M. Haraguchi, and M. Fukui, "Two-dimensionally localized modes of a nanoscale gap plasmon waveguide," Appl. Phys. Lett. **87,** 261114 (2005).
13. R. Zia, M. D. Selker, P. B. Catrysse, and M. L. Brongersma, "Geometries and materials for subwavelength surface plasmon modes," J. Opt. Soc. Am. A **21,** 2442–2446 (2004).
14. M. Lipson, "Guiding, modulating, and emitting light on Silicon - Challenges and opportunities," J. Lightwave Technol. **23,** 4222–4238 (2005).
15. J. A. Dionne, H. J. Lezec, and H. A. Atwater, "Highly confined photon transport in subwavelength metallic slot waveguides," Nano Lett. **6,** 1928–1932 (2006).
16. P. Ginzburg, D. Arbel, M. Orenstein, "Efficient coupling of nano-plasmonics to micro-photonic circuitry," in Conference on Lasers and Electro-optics (Optical Society of America, 2005), paper CWN5.
17. L. Chen, J. Shakya, and M. Lipson, "Subwavelength confinement in an integrated metal slot waveguide on silicon," Opt. Lett. **31,** 2133–2135 (2006).
18. M. Hochberg, T. Baehr-Jones, C. Walker, and A. Scherer, "Integrated plasmon and dielectric waveguides," Opt. Express **12,** 5481–5486 (2004).
19. S. D. Wu, and E. N. Glytsis, "Finite-number-of-periods holographic gratings with finite-width incident beams: analysis using the finite-difference frequency-domain method," J. Opt. Soc. Am. A **19,** 2018–2029 (2002).
20. G. Veronis, R. W. Dutton, and S. Fan, "Method for sensitivity analysis of photonic crystal devices," Opt. Lett. **29,** 2288–2290 (2004).
21. *Handbook of Optical Constants of Solids*, edited by E. D. Palik (Academic, New York, 1985).
22. J. Jin, *The Finite Element Method in Electromagnetics*, (Wiley, New York, 2002).
23. A. Taflove, *Computational Electrodynamics*, (Artech House, Boston, 1995).
24. D. M. Pozar, *Microwave Engineering*, (Wiley, New York, 1998).
25. H. Henke, H. Fruchting, and R. Winz, "Diffraction by a flanged parallel-plate waveguide and a slit in a thick screen," Radio Sci. **14,** 11–18 (1979).
26. J. A. Porto, F. J. Garcia-Vidal, and J. B. Pendry, "Transmission resonances on metallic gratings with very narrow slits," Phys. Rev. Lett. **83,** 2845–2848 (1999).
27. P. Lalanne, J. P. Hugonin, S. Astilean, M. Palamaru, and K. D. Moller, "One-mode model and Airy-like formulae for one-dimensional metallic gratings," J. Opt. A **2,** 48–51 (2000).
28. S. Astilean, P. Lalanne, M. Palamaru, "Light transmission through metallic channels much smaller than the wavelength," Opt. Commun. **175,** 265–273 (2000).
29. Y. Takakura, "Optical resonance in a narrow slit in a thick metallic screen," Phys. Rev. Lett. **86,** 5601–5603 (2001).
30. F. J. Garcia-Vidal, H. J. Lezec, T. W. Ebbesen, and L. Martin-Moreno, "Multiple paths to enhance optical transmission through a single subwavelength slit," Phys. Rev. Lett. **90,** 213901 (2003).
31. M. M. Spuhler, B. J. Offrein, G. L. Bona, R. Germann, I. Massarek, and D. Erni, "A very short planar silica spot-size converter using a nonperiodic segmented waveguide," J. Lightwave Technol. **16,** 1680–1685 (1998).
32. B. Luyssaert, P. Vandersteegen, D. Taillaert, P. Dumon, W. Bogaerts, P. Bienstman, D. Van Thourhout, V. Wiaux, S. Beckx, and R. Baets, "A compact photonic horizontal spot-size converter realized in silicon-on-insulator," IEEE Photon. Technol. Lett. **17,** 73–75 (2005).
33. B. Luyssaert, P. Bienstman, P. Vandersteegen, P. Dumon, and R. Baets, "Efficient nonadiabatic planar waveguide tapers," J. Lightwave Technol. **23,** 2462–2468 (2005).
34. K. Krishnakumar, "Micro-genetic algorithms for stationary and non-stationary function optimization," Proceedings of the SPIE **1196,** 289–296 (1989).
35. B. Wang, J. Jiang, and G. P. Nordin, "Compact slanted grating couplers," Opt. Express **12,** 3313–3326 (2004).
36. P. Koonath, K. Kishima, T. Indukuri, and B. Jalali, "Sculpting of three-dimensional nano-optical structures in silicon," Appl. Phys. Lett. **83,** 4909–4911 (2003).
37. P. Koonath, T. Indukuri, and B. Jalali, "Vertically-coupled micro-resonators realized using three-dimensional sculpting in silicon," Appl. Phys. Lett. **85,** 1018–1020 (2004).

1. Introduction

Plasmonic waveguides have shown the potential to guide subwavelength optical modes, the so-called surface plasmon polaritons, at metal-dielectric interfaces. Several different plasmonic waveguiding structures have been proposed [1, 2, 3, 4, 5, 6], such as metallic nanowires [2, 3] and metallic nanoparticle arrays [4, 5]. Most of these structures support a highly-confined

mode only near the surface plasmon frequency. In this regime, the optical mode typically has low group velocity and short propagation length. It has been shown however that a metal-dielectric-metal (MDM) structure with a dielectric region thickness of $\sim$100 nm supports a propagating mode with a nanoscale modal size at a wavelength range extending from DC to visible [7]. Thus, such a waveguide could be potentially important in providing an interface between conventional optics and subwavelength electronic and optoelectronic devices.

Several different MDM plasmonic waveguide structures have been proposed [8, 9, 10, 11, 12]. In such waveguides the propagation length of the fundamental subwavelength propagating mode is limited by material loss in the metal and is on the order of tens of micrometers at frequencies around the optical communication wavelength ($\lambda_0 =$1.55 μm) [10, 13]. Thus for longer distances it is expected that conventional dielectric waveguides with diffraction-limited optical mode confinement will be used to carry the optical signal. The propagation length in dielectric waveguides is primarily limited by fabrication related disorders and is orders of magnitude larger than the propagation length of MDM plasmonic waveguides [14]. In short, it is expected that MDM waveguides will be used to address subwavelength optoelectronic devices, while conventional dielectric waveguides will be used to transfer the optical signal over distances longer than a few tens of microns. Couplers between MDM and dielectric waveguides will therefore be essential components for most applications involving the use of MDM waveguides such as optical interconnects.

Because of the predicted attractive properties of MDM waveguides, people have started to explore such structures experimentally. In particular, Dionne *et al.* [15] have recently demonstrated waveguiding in a quasi-two-dimensional MDM geometry experimentally, showing clear evidence of a subwavelength guided mode with substantial propagation distances. With this as a background, it is important to explore the coupling of a dielectric slab waveguide into such a quasi-two-dimensional MDM geometry.

In this paper we focus on two-dimensional MDM plasmonic waveguides, and theoretically investigate the coupling of high-index contrast dielectric slab waveguides to such MDM waveguides. We first show somewhat surprisingly that, despite the large difference between the modal sizes of dielectric and MDM plasmonic waveguides, a simple coupler created by placing the dielectric waveguide terminated flat at the exit end of the MDM waveguide without any tapering can be designed to have a transmission efficiency of $\sim$70% at the optical communication wavelength. We then show that the transmission efficiency of the coupler can be increased to 93% by using a 400 nm long multisection taper. In both cases the transmission is found to be broadband. In addition, we investigate the properties of a Fabry-Perot structure in which light is coupled in and out of a MDM waveguide section sandwiched between dielectric waveguides. Finally, we describe a potential fabrication process for such devices. We simulate a structure that could result from such a fabrication process and show that the predicted high transmission efficiency can in fact be observed in that structure.

In previous studies, the coupling between a dielectric slab waveguide consisting of a 1.25 μm silica core surrounded by air, and a 50 nm two-dimensional gold-silica-gold MDM plasmonic waveguide has been theoretically investigated [16]. A coupling efficiency of $\sim$70% was demonstrated by using a 2.5 μm long linearly tapered plasmon waveguide coupler. High coupling efficiency between silicon waveguides and metal slot waveguides using 4 μm long linear tapers has also been demonstrated experimentally [17]. In addition, efficient coupling between silicon-on-insulator dielectric waveguides and metallic stripe plasmonic waveguides has been demonstrated experimentally for a coupling length of 1.8 μm [18]. In contrast, our focus here is on coupling structures either without any transition region between the dielectric and plasmonic waveguides, or with submicron scale transition regions.

The remainder of the paper is organized as follows. In Section 2 we describe the simula-

tion methods used for the analysis of the coupler structures. The results obtained using these methods for the various coupler designs are presented in Section 3. Finally, our conclusions are summarized in Section 4.

2. Simulation method

We use a two-dimensional finite-difference frequency-domain (FDFD) method [19, 20] to theoretically investigate the properties of the couplers. This method allows us to directly use experimental data for the frequency-dependent dielectric constant of metals such as silver [21], including both the real and imaginary parts, with no further approximation. Perfectly matched layer (PML) absorbing boundary conditions are used at all boundaries of the simulation domain [22]. Due to the rapid field variation at the metal-dielectric interfaces, a very fine grid resolution of ∼1 nm is required at the metal-dielectric interfaces to adequately resolve the local fields. On the other hand, a grid resolution of $\sim \lambda/20$ is sufficient in the dielectric waveguide regions of the simulation domain. For example the required grid size in air at $\lambda_0 = 1.55$ μm is ∼77.5 nm which is almost two orders of magnitude larger than the required grid size at metal-dielectric interfaces. We therefore use a nonuniform orthogonal grid [23] to avoid an unnecessary computational cost. We found that by using such a grid our results are accurate to ∼0.05%.

In all cases the dielectric and plasmonic waveguides are aligned with their axes coinciding. To calculate the transmission and reflection coefficients of couplers between dielectric and MDM plasmonic waveguides, we excite the fundamental mode at the input waveguide and measure the power flux at both the input and output waveguides. These fluxes are then normalized with respect to the incident power flux in the input waveguide. We excite the fundamental TM mode of the dielectric waveguide by a line source with the appropriate mode profile calculated by solving the modal dispersion relation. The fundamental TM mode of the MDM plasmonic waveguide can be excited by a single dipole point source, since all higher order modes are well below cutoff for deep subwavelength MDM waveguides.

We define the *transmission efficiency* of the coupler T_{ij} as the ratio of the transmitted power into the fundamental mode of the output waveguide j, and of the incident power of the fundamental mode of the input waveguide i. When the MDM waveguide is the output waveguide, the transmitted power into the MDM waveguide is measured right after the interface of the MDM waveguide with the coupler transition region or with the dielectric waveguide. Similarly, when the MDM waveguide is the input waveguide, the incident power is measured right before the interface of the MDM waveguide with the transition region or with the dielectric waveguide. This definition therefore provides an intrinsic measure of the property of the coupling region only. The presence of material loss, which is included in our simulations, obviously affects this coupling efficiency and is discussed in the next Section. In addition, we note that both the dielectric and plasmonic waveguides considered here support a single guided mode. We always ensure that the output power in the dielectric waveguide side is measured far enough from the interface of the plasmonic and dielectric waveguides, so that the contribution of the radiation modes in the measured power flux is negligible.

We also note that due to reciprocity [24] the transmission efficiency from the dielectric to the plasmonic waveguide T_{dp} is equal to the transmission efficiency from the plasmonic to the dielectric waveguide T_{pd}. However the corresponding reflection coefficients R_{dp} and R_{pd} are not equal, since the power lost to radiation modes in the vacuum depends on whether the input waveguide is the dielectric or the plasmonic waveguide.

3. Results

We first consider a coupler created by simply placing an air-silicon-air dielectric slab waveguide terminated flat at the exit end of a two-dimensional silver-air-silver MDM plasmonic waveguide
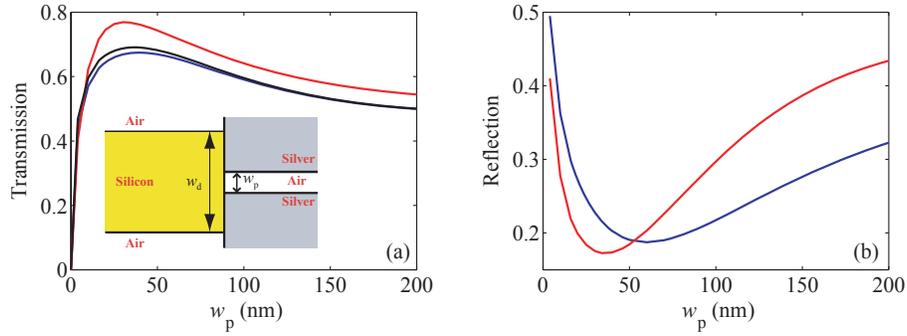
Fig. 1. (a) Power transmission efficiency (blue line) of a coupler between a dielectric and a MDM waveguide as a function of the width of the plasmonic waveguide w_p at $\lambda_0 = 1.55$ μm calculated using FDFD. The coupler, created by placing the dielectric waveguide terminated flat at the exit end of the MDM waveguide, is shown in the inset. Results are shown for $w_d = 300$ nm. Also shown is the transmission efficiency, if the metal in the MDM waveguide is lossless (black line), or perfect electric conductor (red line). (b) Coupler reflection coefficients R_{dp} (blue line), and R_{pd} (red line) as a function of the width of the plasmonic waveguide w_p. All other parameters are as in Fig. 1(a). Experimental data are used for the dielectric constant of the metal, including both the real and imaginary parts.

(inset of Fig. 1(a)). In Fig. 1(a) we show the coupler transmission $T_{dp}(= T_{pd})$ as a function of the width of the plasmonic waveguide w_p at $\lambda_0 = 1.55$ μm. The width of the dielectric waveguide is $w_d = 300$ nm, which approximately corresponds to the optimal width of a silicon slab waveguide surrounded by air that achieves the minimum TM modal size. We observe that the transmission efficiency in this coupler is high and the maximum transmission of 68% is obtained for $w_p \simeq 40$ nm. The transmission is also weakly dependent on w_p for $w_p > 20$ nm. At the limit $w_p \to 0$ the transmission goes to zero as expected. In Fig. 1(a) we also show the transmission for a coupler in which the metal in the MDM waveguide is lossless ($\varepsilon_{\text{met}} = \varepsilon_{\text{met,real}}$, neglecting the imaginary part of the dielectric permittivity $\varepsilon_{\text{met,imag}}$) or perfect electric conductor (PEC) ($\varepsilon_{\text{met}} = -\infty$). In the former case we observe that the material losses in the metal do not affect significantly the transmission efficiency of the coupler. In the latter case (PEC), the transmission of the coupler is slightly higher, and its dependence on the MDM waveguide width is very similar to the plasmonic case. At $\lambda_0 = 1.55$ μm the penetration of the electric field into the metal region is weak, and thus a PEC model provides a reasonable qualitative approximation. In Fig. 1(b) we show the coupler reflection coefficients R_{dp} and R_{pd} as a function of the width of the plasmonic waveguide w_p. The difference between R_{dp} and R_{pd} is due to the presence of radiation loss at the dielectric waveguide side.

In Fig. 2(a) we show the coupler transmission efficiency T_{dp} as a function of the dielectric permittivity ε_p of the gap region of the MDM waveguide. We observe that the transmission T_{dp} is weakly dependent on ε_p. In Fig. 2(b) we show the coupler transmission T_{dp} as a function of the width of the dielectric waveguide w_d for $w_p = 50$ nm, and $w_p = 100$ nm. In this case we observe that the transmission T_{dp} is quite sensitive to w_d. If w_d is decreased below $\sim$300 nm, the modal energy spreads out of the dielectric region. As a result, the modal size of the dielectric waveguide increases rapidly, and the transmission T_{dp} decreases. Similarly for large w_d, the size of the fundamental mode of the dielectric waveguide becomes large and the transmission T_{dp} decreases. If $w_p = 50$ nm ($w_p = 100$ nm), the transmission is maximized for $w_d \simeq 320$ nm ($w_d \simeq 380$ nm).

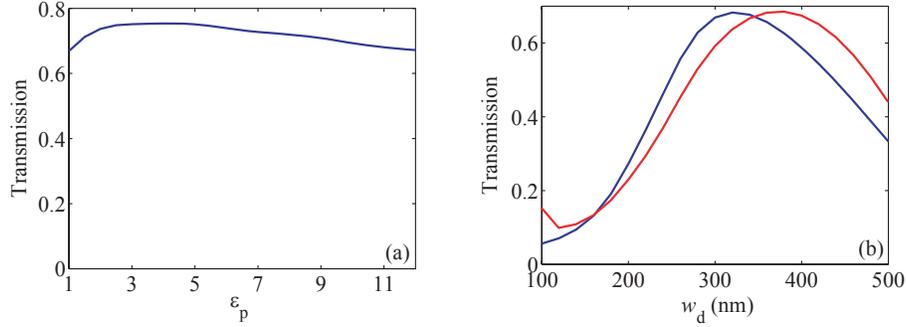In general we found that for a given width of the subwavelength MDM waveguide w_p, there is

Fig. 2. (a) Transmission efficiency as a function of ε_p for $w_p =50$ nm. All other parameters are as in Fig. 1(a). Experimental data are used for the dielectric constant of the metal, including both the real and imaginary parts. (b) Transmission efficiency as a function of w_d for $w_p =50$ nm (blue line), $w_p =100$ nm (red line). All other parameters are as in Fig. 1(a). Experimental data are used for the dielectric constant of the metal, including both the real and imaginary parts.

an optimum width of the dielectric waveguide w_d which maximizes the transmission efficiency and vice versa. We also found that for a given w_d the optimum w_p is significantly smaller than w_d. This is due to the fact that a subwavelength MDM waveguide collects light from an area significantly larger than its cross-sectional area [25]. More precisely, the transmission cross section of a MDM waveguide (in the unit of length in two dimensions), defined as the transmitted power into the waveguide normalized by the incident plane wave power flux, is significantly larger than its geometric cross-sectional area. As an example, we found that the transmission cross section of a MDM waveguide with $w_p =50$ nm is ~185 nm at $\lambda_0 =1.55$ μm. On the other hand, the transmission cross section of dielectric waveguides is approximately equal to their geometrical area. For example, for a waveguide consisting of a silicon slab surrounded by air with $w_d =320$ nm we found that the transmission cross section is ~340 nm at $\lambda_0 =1.55$ μm.

We also note that almost perfect transmittance has been previously reported for metallic grating structures, consisting of a periodic arrangement of subwavelength slits on a metal film [26, 27, 28]. It has also been shown that enhanced transmission is also present in single subwavelength slits [29], and that the transmission can be further enhanced by corrugating the metal surface in the vicinity of the slit [30]. In all these previous studies the transmission was calculated for a plane wave excitation. In contrast, in our case the light funneling is provided by the dielectric waveguide.

In Figs. 3(a) and 3(b) we show the profiles of the magnetic and electric field respectively for a coupler with $w_d =300$ nm, $w_p =50$ nm (Fig. 1(a)). The power is incident from the left so that the incident and reflected waves result in an interference pattern in the dielectric waveguide. We note that the electric field intensity is significantly enhanced in the MDM waveguide with respect to the dielectric waveguide, while similar enhancement is not observed for the magnetic field intensity. This can be understood if we note that from Maxwell's equations we have $E_y = -\frac{1}{j\omega\varepsilon} \frac{\partial H_z}{\partial x} = \frac{\gamma}{j\omega\varepsilon} H_z$, so that for the Poynting vector we have $S = \frac{1}{2}\text{Re}(E_y H_z^*) \propto \frac{\beta}{\omega\varepsilon} |H_z|^2 \propto \frac{\omega\varepsilon}{\beta} |E_y|^2$, where $\gamma = \alpha + j\beta$ is the propagation constant of the mode. Thus, for the magnetic field enhancement we have $|\frac{H_{zp}}{H_{zd}}|^2 \sim \frac{w_d}{w_p} \frac{\beta_d/\varepsilon_d}{\beta_p/\varepsilon_p}$, while for the electric field enhancement we have $|\frac{E_{yp}}{E_{yd}}|^2 \sim \frac{w_d}{w_p} \frac{\varepsilon_d/\beta_d}{\varepsilon_p/\beta_p}$. The observed field enhancements (Fig. 3) are consistent with these relations.

As mentioned above, a simple coupler created by placing a dielectric waveguide terminated flat at the exit end of a MDM waveguide (inset of Fig. 1(a)), can be designed to have transmis-
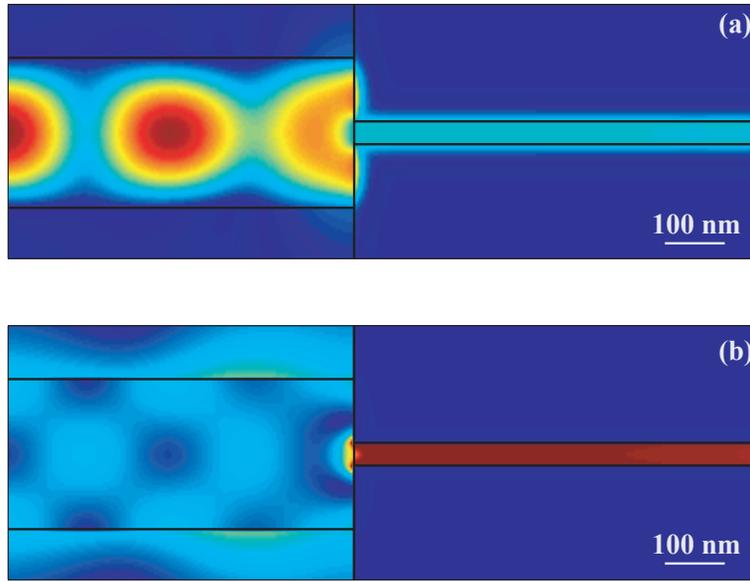
Fig. 3. (a) Profile of the magnetic field amplitude $|H|$ for w_d =300 nm, w_p =50 nm (Fig. 1(a)). (b) Profile of the electric field amplitude $|E|$ for w_d =300 nm, w_p =50 nm.

sion efficiency of 68%. To further increase the transmission, we design a coupler consisting of a multisection taper shown in Fig. 4(a). Such tapers, consisting of a number of waveguide sections, have been used as couplers between dielectric waveguides with highly different widths [31, 32, 33]. It has been shown theoretically and confirmed experimentally that they can be designed to have higher transmission efficiency than conventional tapers of the same length with linear or parabolic shapes [32, 33]. The coupler design used here consists of a number of dielectric waveguide and MDM waveguide sections. The widths of these sections are optimized using a genetic global optimization algorithm in combination with FDFD. More specifically, we use a microgenetic algorithm which has been shown to reach the near-optimal region much faster than large population genetic algorithms [34, 35]. Using this approach we designed a coupler with 93% transmission efficiency for w_d =300 nm, w_p =50 nm at λ_0 =1.55 μm. In this design we use 4 dielectric waveguide sections and 4 MDM waveguide sections. The lengths of all waveguide sections are l_i =50 nm. Their widths $w_1, w_2, ..., w_8$ are optimized using the microgenetic algorithm, while the number of dielectric and MDM sections as well as their lengths are kept fixed during the optimization process. The designed coupler is extremely compact with a total length of 400 nm. The magnetic field profile for this optimized coupler design is shown in Fig. 4(b).

Both the simple coupler of Fig. 1(a) and the multisection taper of Fig. 4(a) were optimized at a single wavelength of λ_0 =1.55 μm. In Fig. 5 we show the transmission efficiency of these couplers as a function of wavelength. We observe that in both cases the transmission efficiency is close to its maximum value in a broad range of wavelengths. This is due to the fact that in both cases the high transmission efficiency is not associated with any strong resonances. Similar broadband responses are observed in couplers between dielectric waveguides with highly different widths based on multisection tapers [32, 33], and in multisection impedance matching transformers used in microwave circuits [24].

In Fig. 6(a) we show a Fabry-Perot cavity structure consisting of a MDM waveguide of length l sandwiched between two dielectric waveguides. In this structure light is coupled from
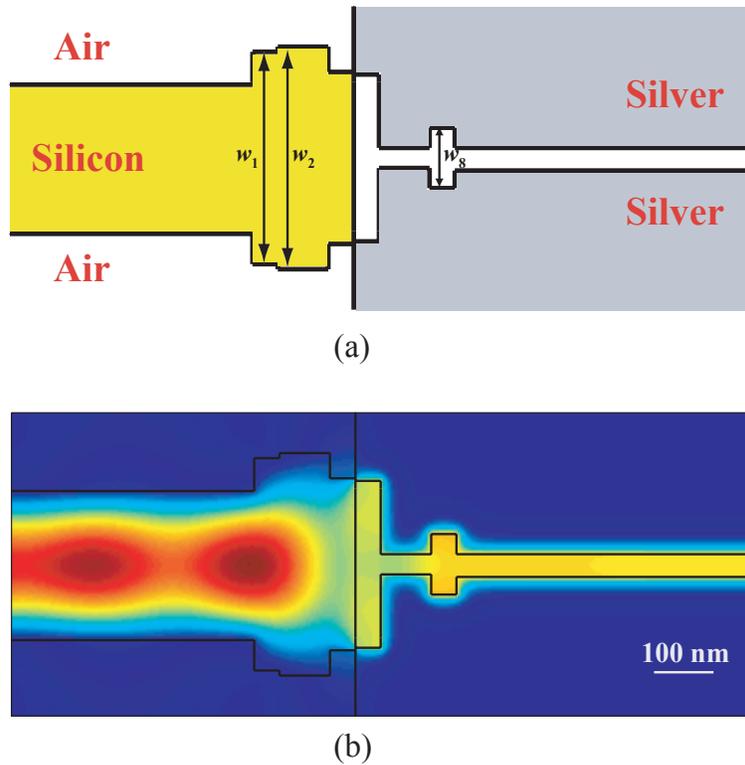
(a)

(b)

Fig. 4. (a) Schematic of a coupler consisting of a multisection taper. (b) Profile of the magnetic field amplitude $|H|$ of the optimized coupler design for w_d =300 nm, w_p =50 nm and 8 waveguide sections. The optimized widths of the dielectric waveguide sections are w_1 =420 nm, w_2 =440 nm, w_3 =440 nm, w_4 =340 nm, while the widths of the MDM waveguide sections are w_5 =330 nm, w_6 =40 nm, w_7 =40 nm, w_8 =120 nm.

the wavelength-sized input dielectric waveguide to a subwavelength MDM waveguide, and then coupled back to the output dielectric waveguide. We excite the fundamental TM mode in the input dielectric waveguide and measure the power coupled into the fundamental mode of the output dielectric waveguide. The transmission efficiency of this structure as a function of the length l of the MDM waveguide section is shown in Fig. 6(b). We observe oscillations typical in the response of a Fabry-Perot structure. Such a device could be potentially used in nonlinear or sensing applications in which the large field enhancement achieved at metal-dielectric interfaces of plasmonic waveguides is desirable. Light could be transfered on chip with low loss dielectric waveguides and coupled efficiently in and out of the plasmonic waveguide-based device.

We also theoretically investigated couplers between silica-silicon-silica dielectric slab waveguides and two-dimensional silver-silica-silver MDM plasmonic waveguides. We note that such a coupler device can be made by first fabricating the dielectric slab waveguide using a Separation by IMplantation of Oxygen (SIMOX) process [36, 37]. Such a process enables the fabrication of silicon/silica waveguiding structures [36, 37]. A portion of the dielectric slab waveguide can then be removed using lithography and etching processes. This step can then be followed by deposition of metal, oxide, and metal layers. Fig. 7 shows a schematic of the proposed structure. We found that if silica (Fig. 7) is used instead of air (Fig. 1) the calculated results for the transmission efficiency are qualitatively the same. We also found that for the
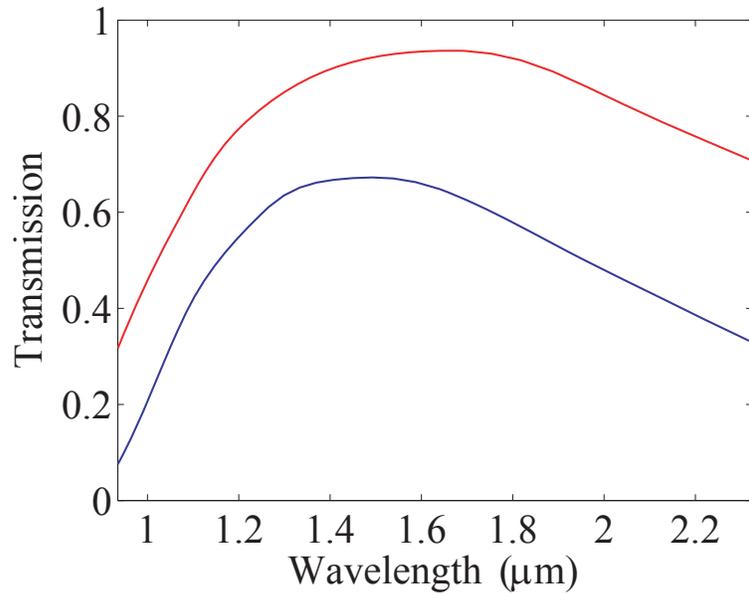
Fig. 5. Transmission efficiency as a function of wavelength for the couplers of Fig. 1(a) (blue line) and Fig. 4(a) (red line). In both cases the coupler parameters were optimized at a single wavelength of $\lambda_0 = 1.55$ μm.
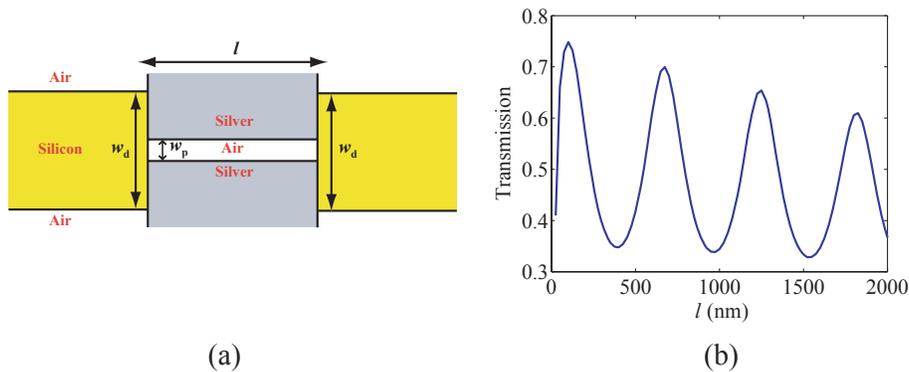

(a)

(b)

Fig. 6. (a) Schematic of a Fabry-Perot cavity structure consisting of a MDM waveguide sandwiched between two dielectric waveguides. (b) Transmission efficiency for the structure of Fig. 6(a) as a function of l at $\lambda_0 = 1.55$ μm. Results are shown for $w_d = 300$ nm, $w_p = 50$ nm.

simple coupler created by placing the dielectric waveguide terminated flat at the exit end of the MDM waveguide very similar high transmission efficiencies are achieved in both the air (Fig. 1) and silica (Fig. 7) cases at the optical communication wavelength.

4. Conclusions

MDM plasmonic waveguide structures can support a propagating mode with a nanoscale modal size over a broad wavelength range. Because of these predicted attractive properties, people have started to explore such structures experimentally. It was recently demonstrated experimen-
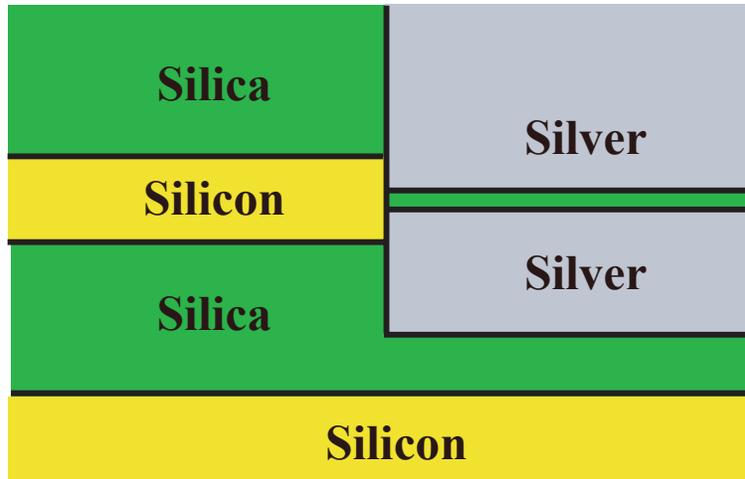
Fig. 7. Schematic of a coupler structure in which a silica-silicon-silica dielectric slab waveguide is coupled to a two-dimensional silver-silica-silver MDM waveguide.

tally that a quasi-two-dimensional MDM waveguide supports a subwavelength guided mode with substantial propagation distance [15]. With this as a background, in this paper we explored the coupling of a dielectric slab waveguide into such a quasi-two-dimensional MDM geometry. We used the FDFD method to theoretically investigate the properties of compact couplers between high-index contrast dielectric slab waveguides and two-dimensional MDM plasmonic waveguides. We first focused on air-silicon-air dielectric slab waveguides coupled to silver-air-silver MDM waveguides. We found that a simple coupler created by placing the dielectric waveguide terminated flat at the exit end of the MDM waveguide can be designed to have a transmission efficiency of ∼70% at the optical communication wavelength. The transmission efficiency of this coupler is strongly dependent on the width of the core of the dielectric waveguide, while it is weakly dependent on the width and the dielectric permittivity of the center layer of the MDM waveguide. We also found that a coupler based on a multisection taper can be designed to have a transmission efficiency of 93% at the optical communication wavelength. The design parameters of the coupler were optimized using a microgenetic optimization algorithm in combination with FDFD. In both the simple coupler and the coupler based on the multisection taper the transmission response was found to be broadband. We also investigated the properties of a Fabry-Perot structure consisting of a MDM waveguide section sandwiched between dielectric waveguides. We showed that the transmission of this structure as a function of the length of the MDM waveguide section exhibits typical Fabry-Perot oscillations. Finally, we investigated couplers between silica-silicon-silica dielectric slab waveguides and silver-silica-silver MDM plasmonic waveguides, which can be fabricated using SIMOX, lithographic, etching, and deposition processes. We found that very similar high transmission efficiencies are achieved in both the air and silica cases. As final remarks, we note that in couplers between three-dimensional dielectric waveguides and MDM plasmonic waveguides there will be additional losses due to out-of-plane light scattering. We are currently investigating whether such couplers between three-dimensional dielectric waveguides and MDM plasmonic waveguides can be designed to have transmission efficiencies as high as the corresponding two-dimensional devices.

Acknowledgments

#76797 - $15.00 USD   Received 6 November 2006; revised 17 January 2007; accepted 17 January 2007

(C) 2007 OSA   5 February 2007 / Vol. 15, No. 3 / OPTICS EXPRESS 1221